Electronic Supplementary Information

Rapid and selective electrochemical transformation of ammonia to N_2 by substoichiometric TiO_2-based electrochemical system

Yanbiao Liu[a,b,*], Jiancheng Mei[a], Chensi Shen[a,b], Manhong Huang[a,b], Ming Yang[c], Zhiwei Wang[b,d], Wolfgang Sand[a,e] and Fang Li[a,b,*]

[a] *Textile Pollution Controlling Engineering Center of Ministry of Environmental Protection, College of Environmental Science and Engineering, Donghua University, 2999 North Renmin Road, Shanghai 201620, P. R. China.*

[b] *Shanghai Institute of Pollution Control and Ecological Security, 1239 Siping Road, Shanghai 200092, P. R. China.*

[c] *Key Laboratory of Cleaner Production and Integrated Resource Utilization of China National Light Industry, Beijing Technology and Business University, Beijing 100048, China.*

[d] *State Key Laboratory of Pollution Control and Resource Reuse, School of Environmental Science and Engineering, Tongji University, Shanghai 200092, China.*

[e] *Institute of Biosciences, Freiberg University of Mining and Technology, Freiberg 09599, Germany.*

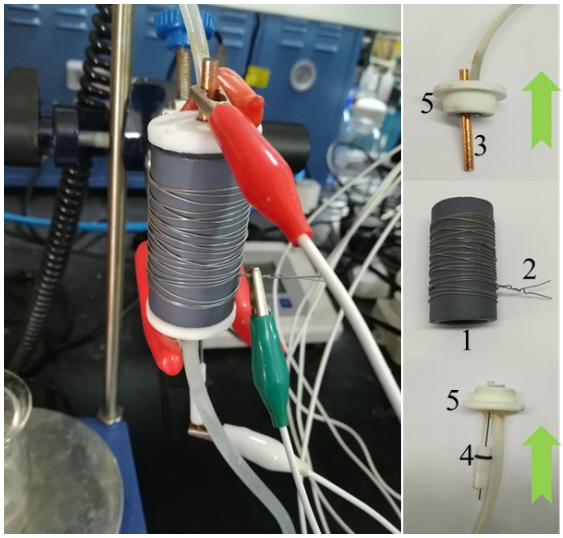

Fig. S1 A digital photograph of the electrochemical system, including 1) a Ti_4O_7 anode, 2) a Ti wire current collector, 3) a carbon rod cathode, 4) a saturated Ag/AgCl electrode, and 5) a silicone rubber.

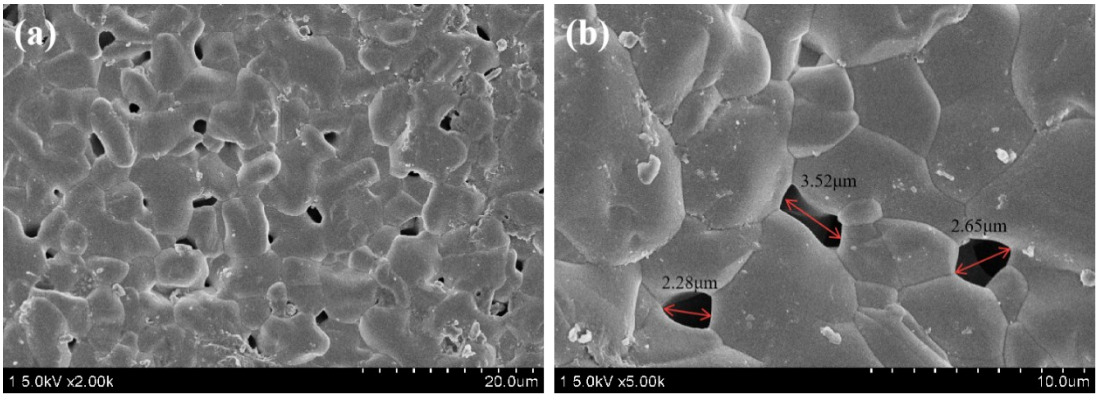

Fig. S2 FESEM images (a, b) of a porous substoichiometric titanium dioxide (Ti_4O_7) tubular electrode.

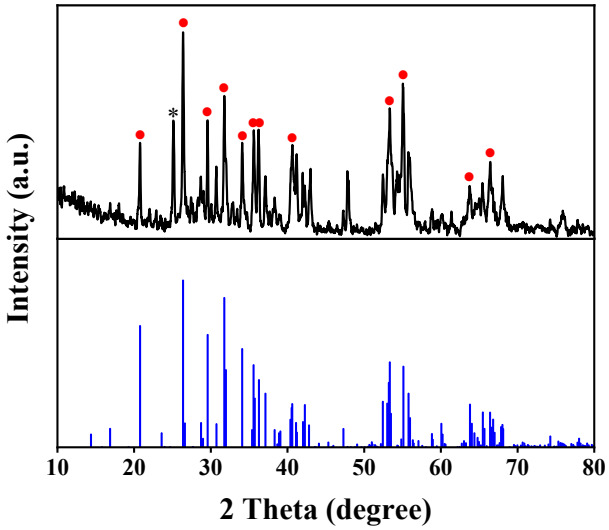

Fig. S3 XRD data of Ebonex® tubular electrode.

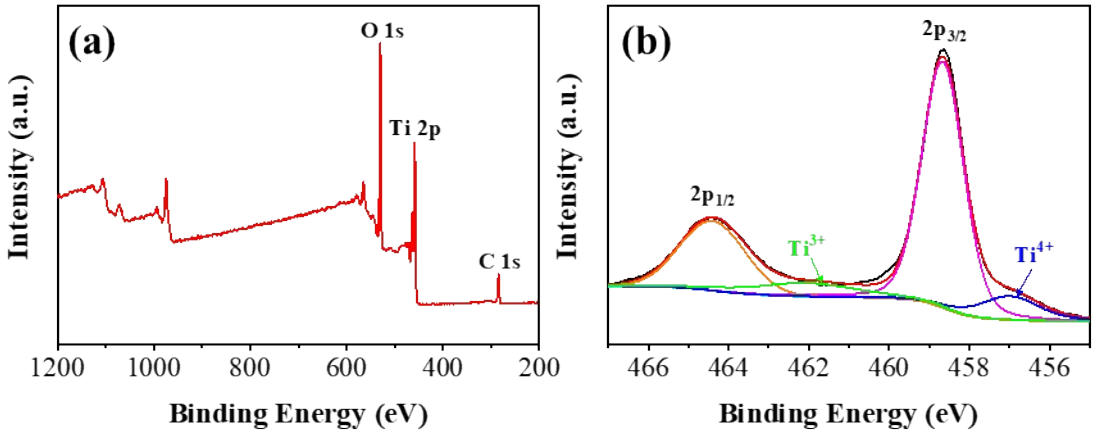

Fig. S4 (a) The wide region scanning XPS spectrum of Ti_4O_7 electrode. XPS spectra for the narrow scan of (b) Ti 2p on Ti_4O_7 electrode.

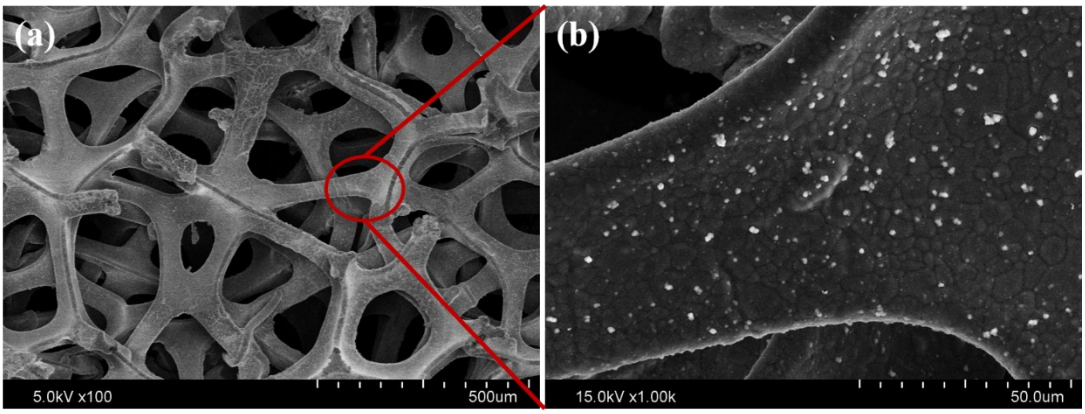

Fig. S5 FESEM images (a, b) of the Pd/Cu-Ni foam electrode.

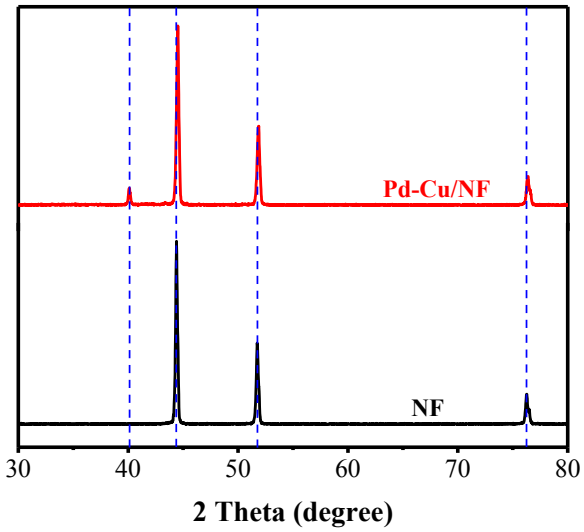

Fig. S6 XRD patterns of the Pd−Cu/NF and NF electrodes.

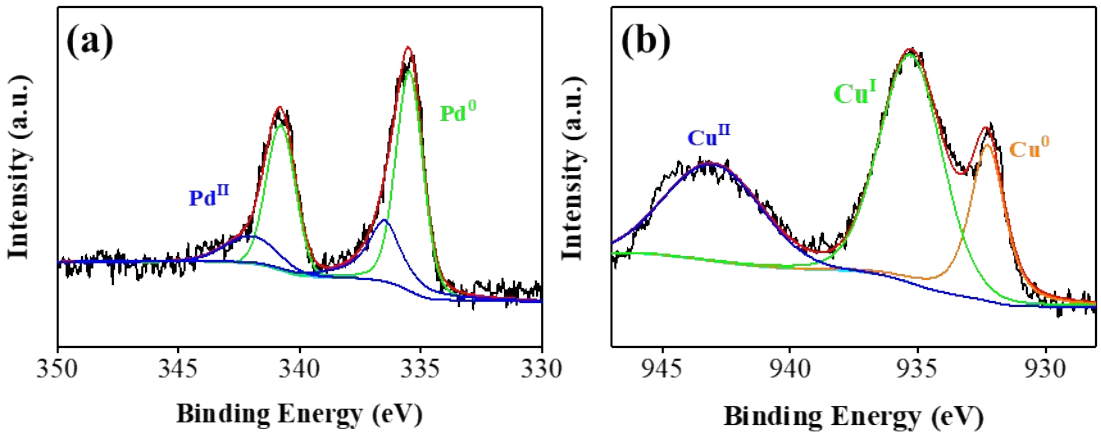

Fig. S7 XPS spectra for the narrow scan of (a) Pd and (b) Cu of a fresh Pd−Cu/NF cathode.

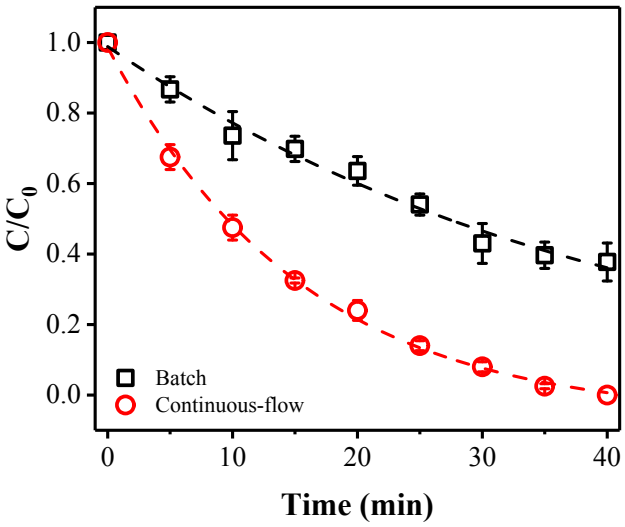

Fig. S8 Comparison of ammonia conversion in batch and continuous-flow systems. Reaction conditions: anode potential of 3.0 V vs. Ag/AgCl, [Cl^-] of 0.12 M, and pH of 7.

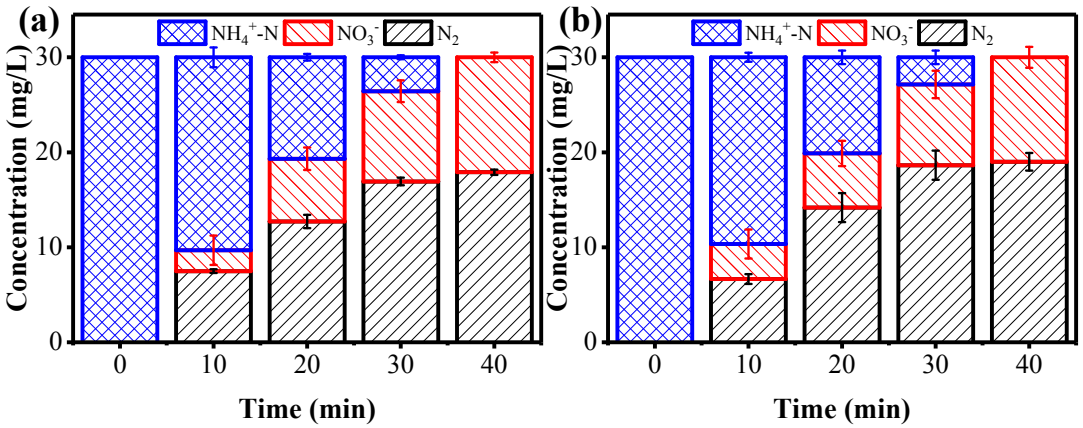

Fig. S9 The conversion of ammonia in 40 min by employing different cathode materials: (a) Pd/NF, and (b) Cu/NF. Reaction conditions: anode potential of 3.0 V vs. Ag/AgCl, [Cl^-] of 0.12 M, flow rate of 4 mL·min^{-1}, and pH of 7.

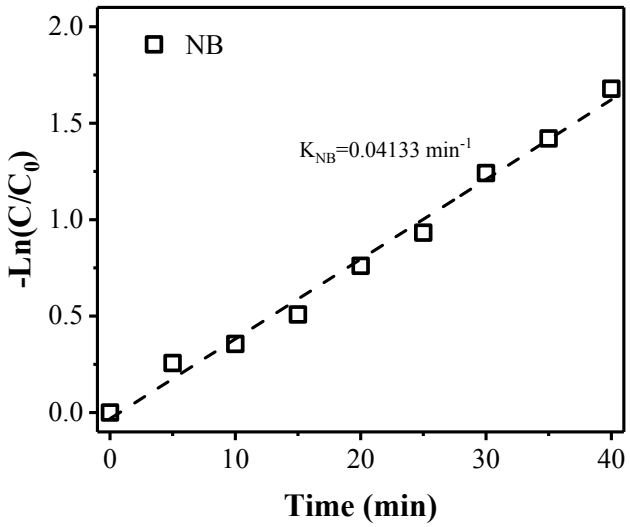

Fig. S10 The plot of $-\ln(C/C_0)$ versus time for the NB degradation.

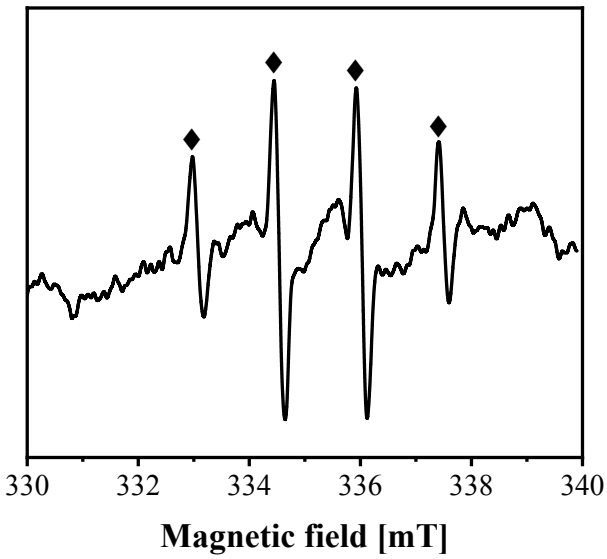

Fig. S11 EPR spectra with DMPO observed from the flow-by experiment after 20 min at an applied anode potential of 3.0 V vs. Ag/AgCl.

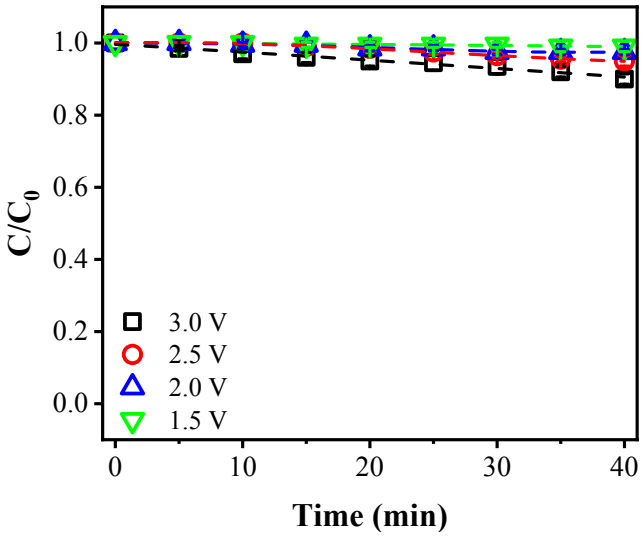

Fig. S12 Conversion effect of ammonia with 0.12 M Na_2SO_4 background electrolyte at different anode potential.

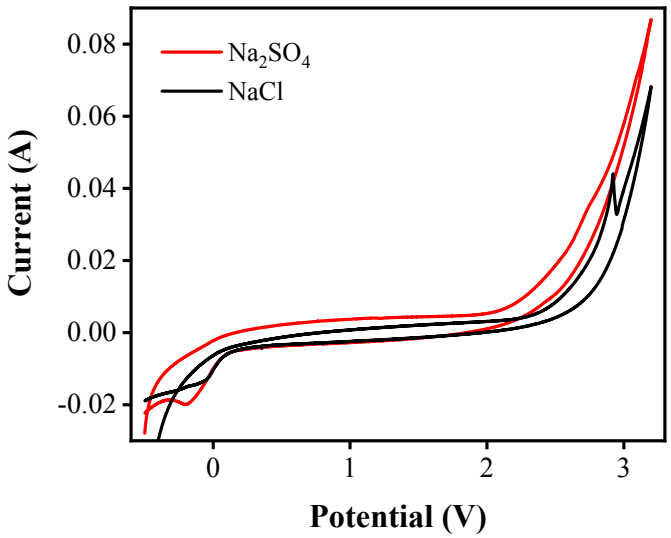

Fig. S13 Cyclic voltammetry results in a 0.12 M NaCl or 0.12M Na_2SO_4 background electrolyte. Scan rate = 20 mV s^{-1}.

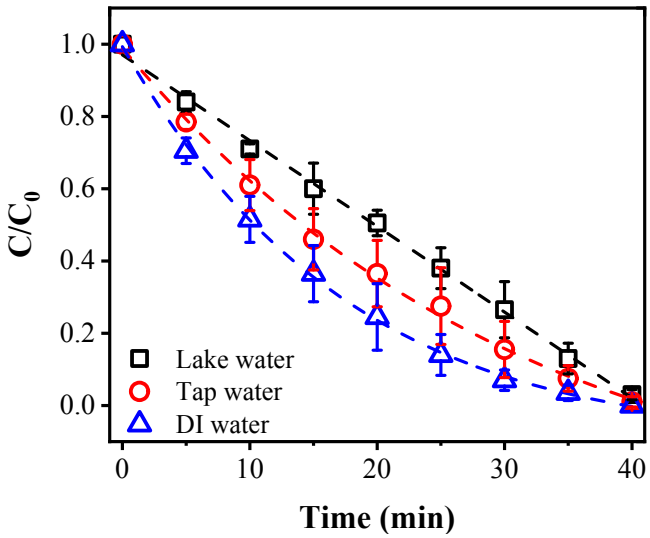

Fig. S14 Impact of background solutions on the ammonia removal. Reaction conditions: ammonia of 30 mg·L^{-1}, anode potential of 3.0 V vs. Ag/AgCl, flow rate of 4 mL·min^{-1}, [Cl$^-$] of 0.12 M, and pH of 7.

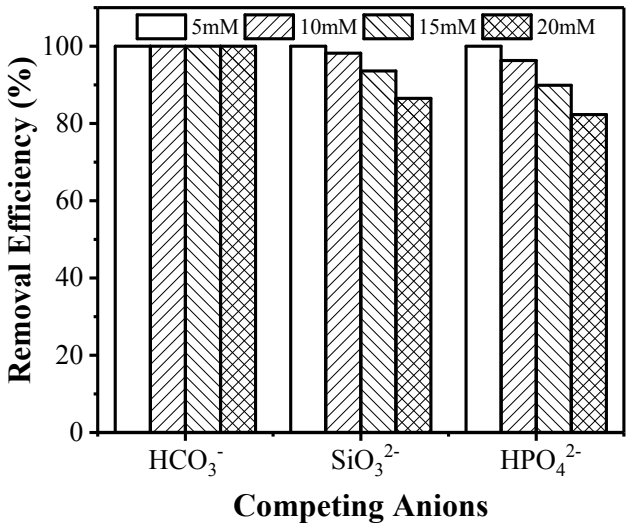

Fig. S15 Effect of competing anions on ammonia conversion.

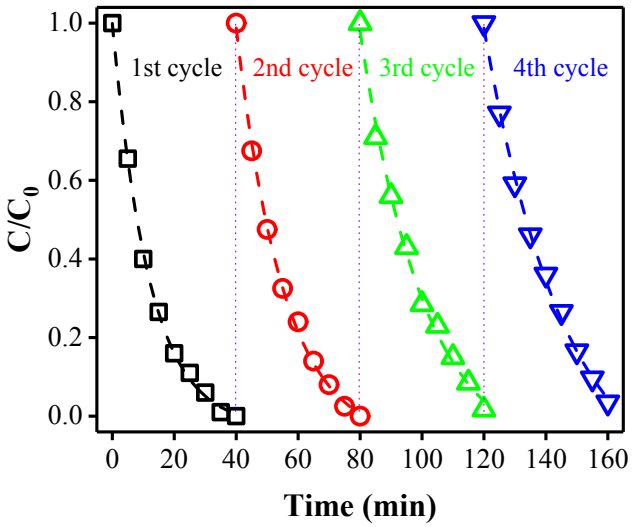

Fig. S16 Comparison of ammonia conversion kinetics during four consecutive cycles. Reaction conditions: ammonia of 30 mg·L^{-1}, anode potential of 3.0 V vs. Ag/AgCl, flow rate of 4 mL·min^{-1}, [Cl^{-}] of 0.12 M, and pH of 7.